

# TERRAIN ECHO PROBABILITY ASSIGNMENT BASED ON FULL-WAVEFORM AIRBORNE LASER SCANNING OBSERVABLES

Werner Mücke<sup>a</sup>, Christian Briese<sup>b</sup>, Markus Hollaus<sup>a</sup>

<sup>a</sup>Institute of Photogrammetry and Remote Sensing, Vienna University of Technology

<sup>b</sup>Christian Doppler Laboratory "Spatial Data from Laser Scanning and Remote Sensing"

Gußhausstraße 27-29, 1040 Vienna, Austria

wm,cb,mh@ipf.tuwien.ac.at

<http://www.ipf.tuwien.ac.at>

**KEY WORDS:** Vegetation, LIDAR, analysis, classification, laser scanning, estimation

## ABSTRACT:

Airborne laser scanning (ALS) has become a widely used method for data acquisition in various fields of engineering over the past few years. The latest generation of commercially available ALS systems, the so-called full-waveform ALS systems, are capable of detecting the whole backscattered waveform, which needs to be analysed in post-processing in order to detect the individual echoes. During this signal processing step additional observables, such as the amplitude and the width of the backscattered echo, are derived. The hereby produced 3D point cloud holds additional information about the radiometric and geometric characteristics of the objects within the footprint area of the laser beam. In this paper point cloud samples of different ground cover are examined regarding their distribution of amplitude and echo width. Subsequently, a method for employing these observables for the assignment of probabilities, whether an echo is more likely to stem from terrain or not, is presented. These probabilities can also be interpreted as individual weights that are assigned to the single points and can be used in subsequent digital terrain modelling (DTM) algorithms for a derivation of more accurate DTMs.

## 1 INTRODUCTION

The sampling of the earth's surface with laser technology for obtaining information about its geometric structure has become an efficient and wide-spread method for data acquisition over the past few years. 3D point clouds from airborne laser scanning (ALS), which is also referred to as airborne LiDAR (light detection and ranging), provide a data basis for various applications and have been used in different fields of engineering, such as forestry (Hyypä et al., 2008; Naesset, 2007), urban monitoring (Dorninger and Pfeifer, 2008; Höfle et al., 2009), hydrology (Mandlbürger et al., 2009; Briese et al., 2009; Höfle et al., 2009) or archaeology (Doneus et al., 2008).

Most of the above mentioned applications have in common that they rely on an accurate digital terrain model (DTM), derived on the basis of the point cloud. The quality of the DTM itself is, among other influencing factors (Kraus et al., 2004), dependent on the reliability to eliminate off-terrain echoes (Kraus et al., 2004; Karel et al., 2006). Conventional methods for classifying the point cloud into terrain and off-terrain echoes, a process also called filtering, employ various geometric criteria. This might be the distance to prior computed surfaces (Axelsson, 2000; Kraus and Pfeifer, 1998; Pfeifer et al., 2001), relations of planimetric distance and height difference (Vosselman, 2000) or normal vectors as a homogeneity criteria in a segmentation based approach (Tóvari and Pfeifer, 2005). However, reflections from near terrain objects, e.g. lower under storey, cannot be distinguished by geometric criteria alone. Especially near ground vegetation poses two problems. The first problem concerns the range resolution. If the vegetation is very low, the range difference between two consecutive targets may become too short for the detector to separate them. Consequently, only one target is identified, which features a measured distance that results from an overlap of the two actual reflections. The resulting point is then located somewhere in between them (Kraus, 2007). Secondly, areas with dense vegetation feature only little to no penetration at all. This is crucial if the trend of the surface changes significantly below the impenetrable

vegetation and no echoes from the terrain are detected. In both cases, echoes tend to be wrongly classified as ground points. Consequently, a DTM surface computed on the basis of a point cloud including such off-terrain echoes, might run through the lowest vegetation levels and therefore above the actual terrain. As these errors can be in the range of several decimetres, they are critical for DTM based application where high accuracy is required (Doneus et al., 2008).

Currently, two different types of ALS sensors, which can be distinguished by their method of echo detection, are commercially available. The so-called discrete recording systems are able to record the range and amplitude of one or more consecutive discrete echoes. In contrast, the so-called full-waveform (FWF) digitizers, are capable of detecting and storing the whole emitted and backscattered signal. To then obtain the individual echoes, the recorded waveform has to be reconstructed in post-processing and a decomposition algorithm, which can be individually adapted, has to be applied. Recent papers describe different methods for ALS waveform analysis and echo detection (Wagner et al., 2006; Roncat et al., 2008; Mallet et al., 2009). During the process, the echoes are detected and the range of the scanner to the target, as well as additional variables are derived. In addition to the amplitude, the width of the backscattered signal, also commonly known as the echo width, is determinable.

The usage of these additional observables opens up new prospects for DTM generation from ALS data, although very rarely used so far. Wagner et al. (2008) stated that the width of the backscattered echo is dependent on the vertical distribution of small surface elements within the footprint area of the laser beam. The canopy, under storey or near ground vegetation are assumed to have larger variations in vertical directions and consequently larger echo widths than the terrain. Based on this fact, Doneus et al. (2008) used an empirically derived echo width threshold, pre-classifying presumable off-terrain echoes in the input point cloud for the hierarchic robust filtering (Pfeifer et al., 2001). In Lin and Mills (2009), a point labelling process, determining terrain points us-

ing a threshold for the echo width is applied to complement the individual 3D points. This additional surface information is integrated in a DTM generation approach employing Axelsson's progressive densification method (Axelsson, 2000).

However, applying hard thresholds on datasets poses several difficulties. On the one hand, the derived thresholds are always sensor specific and do not necessarily apply for others. On the other hand, the above mentioned strategies tend to eliminate a certain number of points based on a-priori determined thresholds. This implies the possibility of creating false negatives, meaning excluding reflections that might very well stem from terrain. These echoes are permanently lost for subsequent filtering steps.

The method described in this paper considers these limitations and disadvantages of pre-classifying echoes based on a fixed echo width threshold. Rather than using thresholds on either one of the FWF-observables (amplitude and echo width), it focuses on the modelling of the distribution of the echo widths dependent on amplitude values. As for the derivation of a DTM only the last echoes are relevant, probabilities indicating whether they are more likely to be a terrain echo or not are assigned to the echoes. These probabilities can be interpreted as individual weights and can be used as a-priori weights in existing filtering algorithms. Hence, the whole point cloud is preserved and augmented with additional information, which can subsequently be used for a more accurate derivation of DTMs.

In the following section 2 the study area is described. Section 3 deals with the theoretical background of the proposed method (see section 3.1), a description of the point cloud analysis (see section 3.2) and the probability assignment (see section 3.3). Finally, the results are summarized and discussed in section 4 and a conclusion is given in section 5.

## 2 STUDY AREA AND DATA

An ALS data set collected over the city of Eisenstadt, capitol of county Burgenland, Austria, was used in this paper. As study area a small sample within the Schlosspark Eisenstadt was created. The ALS data were acquired under leaf-off conditions in March 2007. A RIEGL LMS-Q560 laser scanner, which is equipped with a full-waveform recorder, was employed. The main technical specifications can be found on the distributors website (Riegl, 2009a). The scanner was carried by a fixed-wing aircraft as well as a helicopter alternatively, which operated at an average flying altitude of 600 m, the scan angle was set to  $\pm 22.5^\circ$  and the average distance of the single trajectories was 90 m. This resulted in a large overlap of the ALS strips and, consequently, rather high point density of 18 echoes per  $m^2$  for the whole data set. Using Gaussian decomposition, as described in Wagner et al. (2006), the single echoes were extracted from the raw waveform data and a 3D point cloud was obtained. For adequate geo-referencing the method proposed by Kager (2004) was applied. This process allows to reduce discrepancies between overlapping ALS strips. The produced high quality 3D point cloud was then used to derive a digital surface model (DSM) utilizing moving planes interpolation. Furthermore, a DTM using hierarchic robust interpolation (Pfeifer et al., 2001) was generated. Both methods are implemented and documented in the software package SCOP++ (SCOP++, 2008). The DTM was used to compute the normalized heights of the single echoes for point selection and later verification purposes. A hill-shading of the study area can be seen in figure 1a. The obtained point cloud consisted of 57.3% single echoes (only one reflection in the shot), 27.8% shots with two, 11.8% with three 2.7% with four and 0.4% with more than four consecutive target reflections.

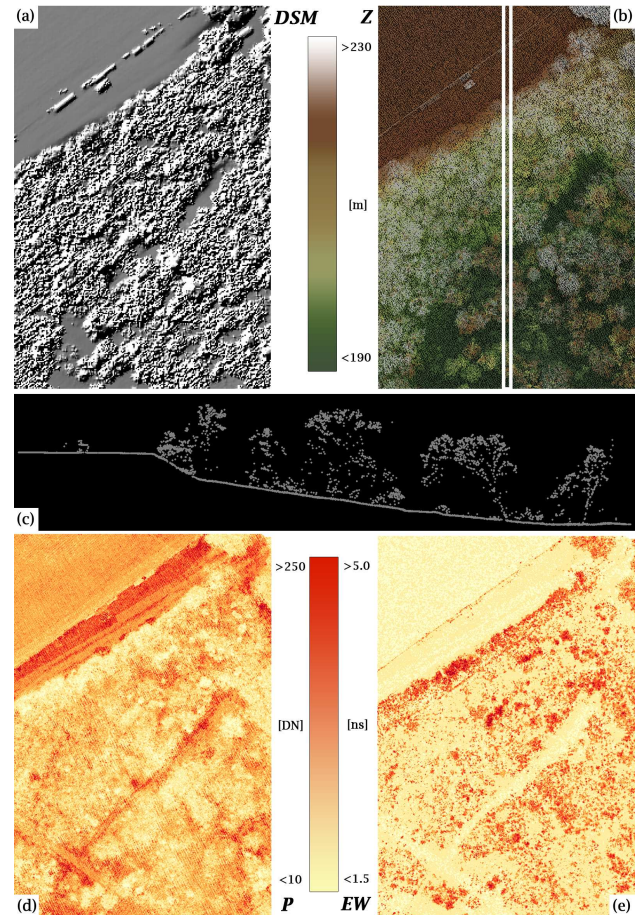


Figure 1: ALS study area in Schlosspark Eisenstadt (120 x 170 m). (a) DSM (grid size 0.25 x 0.25 m) created of all echoes; (b) height-coded point cloud showing all echoes (Z), white bars indicate location of profile; (c) profile; (d) amplitudes (P) of the last echoes; (e) echo widths (EW) of the last echoes.

## 3 METHOD

### 3.1 Theoretical Background

As written in section 1 and based on Wagner et al. (2008), the echo width provides information about the height distribution of small scatterers within the footprint area of the laser beam. A planar area, perpendicular to the laser beam direction, features no height variation at all. It is therefore assumed that a laser beam impinging approximately rectangular on such terrain should cause a backscattered signal with an echo width equal or similar to the width of the emitted pulse (Wagner et al., 2004). According to its specifications, the RIEGL LMS-Q560 laser scanner emits pulses with a duration of 4 ns, describing the full width of the pulse at its half maximum (FWHM). It has to be stated that due to the utilized software for echo extraction, the derived echo widths do not represent the FWHM, as it is common practice in signal processing and commercial software (e.g. Riegl (2009b)), but the standard deviation of the fit Gaussian curve. The width of the emitted pulse has to be divided by a constant factor of

$$2 * \sqrt{2 * \ln 2} = 2.3548 \quad (1)$$

in order to correspond to the echo widths derived by the applied echo extraction method, which results in a value of 1.6986 ns (Mücke, 2008).

Examination of the echo width image in figure 1e supports this theory. In the north-western corner a football court is located,

which is a flat non-tilted plane featuring also the lowest echo widths of about 1.75 ns in the sample area. The pathway through the forest (centre of the image), which is not overgrown by trees, also shows reflections of comparable widths. The largest echo widths in the area stem from vegetation echoes, characterized by values well above 2 ns and up to 5 ns. Also the lower amplitude values can be found in the vegetated area (see figure 1d). This is probably the result of a potentially higher number of consecutive echoes in the penetrable canopy and multi-layered vegetation below. The more reflections per shot, the less energy can be scattered back by the individual targets and consequently the last echoes feature the lower amplitude values (Wagner et al., 2008).

### 3.2 Point cloud analysis

To confirm our assumption, single echoes from open terrain areas were selected and scatter plots showing their amplitudes and respective echo widths were produced (see figure 2). Compared to the width of the emitted pulse (dotted blue line in figure 2), the four samples, taken from reflections over gravel (1452 points), sand (1059 points), asphalt (1427 points) and grassland (4628 points), seem to correspond quite well. Except for a minimal positive shift with respect to the width of the emitted pulse and increased scattering of the echo widths with decreasing amplitude values. This scattering was also observed by Wagner et al. (2006), explained as a characteristic of FWF decomposition using a Gaussian model. They stated that the method is robust for strong echoes and becomes less reliable for weak ones. Subsequently, we examined if the amplitudes and widths of single and last echoes from forest terrain behave similar as the ones from open terrain. Figure 3 shows a scatter plot produced from reflections of an overgrown area. They were selected using the previously calculated normalized heights ( $dZ$ ) with respect to the DTM and a  $dZ \leq 0.2$  m threshold (see section 2), so they approximate the terrain as good as possible. We found that the 0.2 m threshold was adequate given the definition uncertainty of a forest terrain covered by fallen leaves, tree roots and creepers of any kind. Further reducing the threshold did not significantly minimize the resulting terrain point cloud, whereas an increase to 0.5 m had the opposite effect. By visual comparison we examined that lots of points representing relevant near terrain vegetation were included.

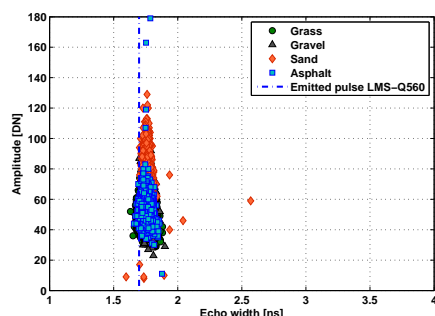


Figure 2: Scatter plot of selected single echoes from open terrain (grass, gravel, sand, asphalt); width of the emitted pulse is shown by dotted blue line.

### 3.3 Probability Assignment

We expect the scatter plot in figure 3 to depict the distribution for amplitudes and echo widths of terrain echoes in vegetated areas and base the probability assignment on this assumption. First, a distribution function dependent on the amplitudes and respective echo widths is created. It is fit to the distribution on the left side

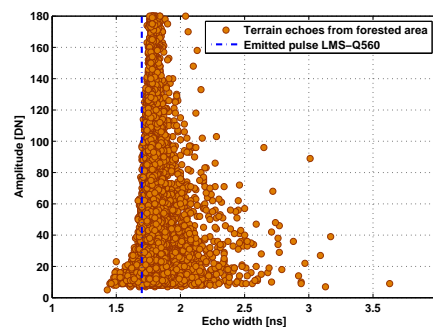


Figure 3: Last echoes from forest terrain selected by height thresholding ( $dZ \leq 0.2$  m); width of the emitted pulse is shown by the dotted blue line.

of the median of the echo widths, because there the detection accuracy we can expect from the applied Gaussian decomposition is demonstrated. We then flip the function vertically along the median (see figure 4), so the two functions combined now outline the range of amplitude and echo width values for reflections that stem from terrain with a high probability. 3D points within this area are given the highest weights, which is defined as 95% (green zone in figure 4). As we do not expect a shortening of the echo widths due to vegetation but rather the opposite, every echo left of the area outlined by the distribution function (green zone) is given the lowest weight of 5%. In order to avoid hard thresholds in the transition from high to low weight, we defined a buffer zone along the flipped curve. Inside of it a linear function is used for applying the individual weights, ranging from 95% to 5%. Every point outside the transition zone is considered not to represent terrain and is therefore given the lowest weight (5%). This method tends to give the highest weights to points belonging to terrain with a high probability, points assumed to be off-terrain echoes gain the lowest weights.

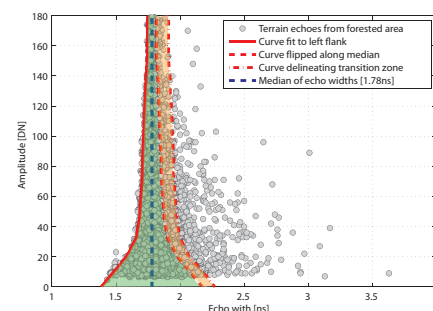


Figure 4: Last echoes from forest terrain; fit distribution function (red lines); highest weights  $w = 95\%$  (green), transition zone  $95\% < w < 5\%$  (orange), lowest weights  $w = 5\%$  are assigned outside the green and orange zones.

## 4 RESULTS AND DISCUSSION

The distribution of the forest terrain echoes (figure 3) shows similar characteristics as the one from the open terrain echoes (figure 2). The scattering of the echo widths also increases with decreasing amplitudes. However, it features echoes with very low amplitudes, which are not present in the single echoes from open terrain and can be explained by the persistent loss of energy due to the detection of consecutive targets in the vegetated area. Also the echo widths cover a wider range up to 3 ns, indicating that some of the selected terrain points represent rough surfaces, e.g.

points on tree roots or stems. Apart from that a slight shift compared to the emitted pulse is recognizable in all of the produced point cloud samples. At this time the cause of this shift is uncertain. Probably the incidence angle of the laser shot might influence the echo width, causing it to become wider with small (acute) angles. Essentially, this corresponds to a widening of the reflected signal caused by height variation. However, the examined echoes stemming from open areas represent near horizontal terrain (e.g. left part of profile in 1c representing the football court) and are located in the middle of the strip, roughly below the trajectory of the flight. So the angle of deflection is small and consequently the incidence angles are rather obtuse, a change of the echo widths caused by this is therefore unlikely. Another reason could be that the width of the emitted pulse is not constantly 4 ns, but sometimes wider, subsequently causing bigger echo widths in the backscattered signals. But to our knowledge this has not been explored so far.

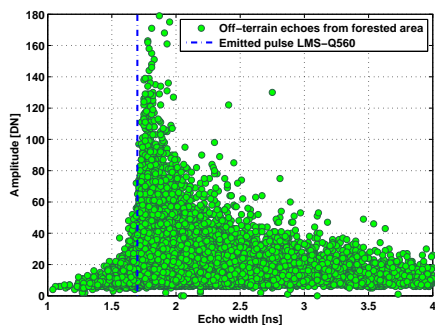


Figure 5: Off-terrain echoes from a forested area selected by height thresholding (last echoes  $dZ > 0.2$  m); width of the emitted pulse is shown by dotted blue line.

Further, the distribution function derived in section 3 (figure 4) was compared to the scatter plot of the selected off-terrain last echoes in the forested area (see figure 5), which were generated by height thresholding ( $dZ > 0.2$  m) as well. Although there is a large overlap, the distribution is very asymmetric and shifted towards higher echo widths, featuring a significant amount of echoes we can expect to be given the lowest weight.

Consequently, the distribution function was used to assign weights to the single and last echoes within the study area, because these are usually the lowest points and therefore considered to represent terrain. For a validation of the results the afore calculated normalized heights were employed. Initially we selected terrain points in the forested area by applying a threshold of 0.2 m ( $dZ \leq 0.2$  m) (see section 3.2) on the normalized heights of the single and last echoes. We repeated that for our study area (see figure 1), producing a terrain point cloud that consisted of 184868 points, starting from a total of 226767 points. Comparing this number to the number of points that were assigned weights of  $w = 95\%$ , we found that 92% of the terrain echoes selected by height thresholding were given the maximum weight ( $w = 95\%$ ). Additionally, we extracted the echoes that gained the maximum weight and those that gained less ( $w < 95\%$ ) and produced a histogram of the normalized heights (see figure 6). It clearly reveals that more than 80% of the echoes with maximum weight are located below 0.5 m. Apart from that, 7.1% of the points with weights of less than 95% (points that are unlikely to stem from terrain) are also in that height range. More detailed investigations and visual examinations have shown that these echoes stem from lower vegetation or tree stems, therefore also being correctly weighted. This explanation is supported by figure 7b, where the low weighted echoes

( $w < 95\%$ ) color-coded by their respective normalized height  $dZ$  are shown. The points are within the dark green area feature normalized heights of 0.5 m and below.

The remaining part of the single and last echoes, featuring high as well as low weights, are spread over the entire range of normalized heights occurring in our study area. This points out a limitation of the probability assignment, which is partly rooted in the applied echo detection method. The lower the amplitude, the higher the tolerance for points gaining maximum weight. Strong first echoes in the canopy might have large echo widths and be therefore correctly weighted. However, for consecutive echoes less energy is left (Wagner et al., 2008), and thus, as we have already pointed out in section 1, the echo width estimation becomes less trustworthy. This probably results in reflections from branches and stems high above the terrain having smaller echo widths, although they represent rather rough surfaces. For this reason they are wrongly given high weights. Figure 7a shows

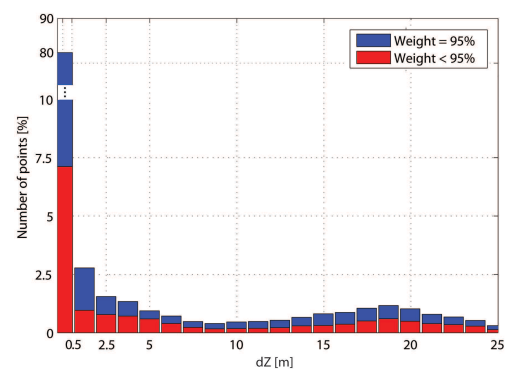


Figure 6: Histogram of single and last echoes from sample area. Points that were weighted with 95% (blue) and less than 95% (red).

the points with a weight of  $w = 95\%$ . The white square outlines echoes in the canopy ( $dZ > 20$  m). The apparent explanation for these points being given the maximum weight is that the dense canopy acts as a single scatterer, featuring too little height variation within the footprint of the laserscanner to be detected. Consequently, they have similar characteristics as terrain echoes. The same applies for thick branches of trees or stems with large diameters, which can also be seen as extended targets (Jelalian, 1992), meaning they are bigger than the footprint size. However,

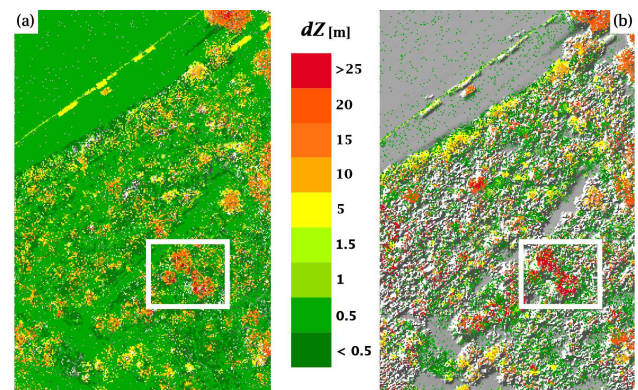


Figure 7: (a) DSM overlay with single and last echoes featuring maximum weights  $w = 95\%$  (b) DSM overlay with single and last echoes featuring weights  $w < 95\%$ . The white square shows the area with dense canopy.

these points do not pose a problem for conventional filtering algorithms, as they are well elevated and can be reliably detected and

eliminated by the geometric analysis of the local neighbourhood. As pointed out in section 1, it is rather the near ground vegetation that causes troubles in DTM generation and the proposed classification method has proven to be valuable in the detection of reflections from such objects.

## 5 CONCLUSIONS AND FUTURE WORK

Our investigations have demonstrated that the full-waveform observables amplitude and echo width have potential for the assignment of probabilities whether an ALS point represents terrain or not. The suggested method managed to label 92% of the terrain echoes correctly (see section 4) and additionally correctly detected reflections from near ground vegetation. However, we found that the approach can not produce exclusive terrain point clouds, given the fact that amplitude and echo width are metrics that do not discriminate sufficiently to do so. A reliable determination of off-terrain points without the utilization of geometric criteria seems rather difficult. But as presented in other papers (Briese et al., 2007; Lin and Mills, 2009), conventional filtering methods profit from a-priori separated vegetation echoes which could be found with the help of full-waveform observables. The approach proposed in this paper produces a point cloud enriched by individual weights for each point, which can now be used in subsequent filtering steps. In our further work we will concentrate on the integration of the individual weights into the hierarchic robust interpolation. Apart from that we plan on acquiring a proper reference dataset with terrestrial laser scanning which we will use for the derivation of a very detailed and highly accurate DTM to compare it to the ALS DTM and adequately validate the employed filtering method.

## ACKNOWLEDGEMENTS

The authors would like to thank Michael Doneus, Department for Prehistory and Early History of the University of Vienna, Austria, for providing the used ALS data set. Further we would like to thank Andreas Roncat for fruitful discussions. This study was partly funded by the TransEcoNet project implemented through the CENTRAL EUROPE Program co-financed by the ERDF.

## References

- Axelsson, P., 2000. DEM generation from laser scanner data using adaptive TIN models. In: *International Archives of Photogrammetry and Remote Sensing*, XXXIII, B4, Amsterdam, Netherlands, pp. 111–118.
- Briese, C., Doneus, M., Pfeifer, N. and Melzer, T., 2007. Verbesserte DGM-Erstellung mittels full-waveform airborne Laserscanning. In: *3-Ländertagung DGPF, SGPBF, OVG, Basel*.
- Briese, C., Mandlbürger, G. and Ressel, C., 2009. Automatic break line determination for the generation of a dtm along the river main. In: *ISPRS Workshop Laserscanning 2009, Paris, FRANCE*.
- Doneus, M., Briese, C., Fera, M. and Janner, M., 2008. Archaeological prospection of forested areas using full-waveform airborne laser scanning. *Journal of Archaeological Science* 35(4), pp. 882–893.
- Dorninger, P. and Pfeifer, N., 2008. A comprehensive automated 3d approach for building extraction, reconstruction, and regularization from airborne laser scanning point clouds. *Sensors* 8(11), pp. 7323–7343.
- Höfle, B., Mücke, W., Dutter, M., Rutzinger, M. and Dorninger, P., 2009. Detection of building regions using airborne lidar - a new combination of raster and point cloud based gis methods. In: *Geospatial Crossroads at GI-Forum 09 – Proceedings of the Geoinformatics Forum Salzburg*.
- Höfle, B., Vetter, M., Pfeifer, N., Mandlbürger, G. and Stötter, J., 2009. Water surface mapping from airborne laser scanning using signal intensity and elevation data. *Earth Surface Processes and Landforms* 34(12), pp. 1635–1649.
- Hyypä, J., Hyypä, H., Leckie, D., Gougeon, F., Yu, X. and Maltamo, M., 2008. Review of methods of small-footprint airborne laser scanning for extracting forest inventory data in boreal forests. *International Journal of Remote Sensing* 29(5), pp. 1339–1366.
- Jelalian, A. V., 1992. *Laser Radar Systems*. Artech House, Boston.
- Kager, H., 2004. Discrepancies between overlapping laser scanning strips - simultaneous fitting of aerial laser scanner strips. In: *International Archives of Photogrammetry and Remote Sensing*, XXXV, B/1, Istanbul, Turkey, pp. 555–560.
- Karel, W., Briese, C. and Pfeifer, N., 2006. Dtm quality assessment. In: *International Archives of Photogrammetry and Remote Sensing*, XXXVI, 2, Vienna, Austria.
- Kraus, K., 2007. *Photogrammetry – Geometry from Images and Laser Scans*. 2 edn, de Gruyter.
- Kraus, K. and Pfeifer, N., 1998. Determination of terrain models in wooded areas with airborne laser scanner data. *ISPRS Journal of Photogrammetry and Remote Sensing* 53, pp. 193–203.
- Kraus, K., Briese, C., Attwenger, M. and Pfeifer, N., 2004. Quality measures for digital terrain models. In: *International Archives of Photogrammetry and Remote Sensing*, XXXV, B2, Istanbul, Turkey, pp. 113–118.
- Lin, Y. and Mills, J., 2009. Integration of full-waveform information into the airborne laser scanning data filtering process. In: *Laser Scanning 2009, Paris*.
- Mallet, C., Lafarge, F., Bretar, F., Roux, M., Soergel, U. and Heipke, C., 2009. A stochastic approach for modelling airborne lidar waveforms. In: F. Bretar, M. Pierrot-Deseilligny and G. Vosselman (eds), *Laserscanning 2009 – International Archives of the Photogrammetry, Remote Sensing and Spatial Information Sciences XXXVIII, Part 3/W8*, pp. 201–206.
- Mandlbürger, G., Hauer, C., Höfle, B., Habersack, H. and Pfeifer, N., 2009. Optimisation of lidar derived terrain models for river flow modelling. *Hydrology and Earth System Sciences* 13(8), pp. 1453–1466.
- Mücke, W., 2008. Analysis of full-waveform airborne laser scanning data for the improvement of DTM generation. Master's thesis, Institute of Photogrammetry and Remote Sensing, Vienna University of Technology.
- Naesset, E., 2007. Airborne laser scanning as a method in operational forest inventory: Status of accuracy assessments accomplished in scandinavia. *Scandinavian Journal of Forest Research* 22(5), pp. 433–442.
- Pfeifer, N., Stadler, P. and Briese, C., 2001. Derivation of digital terrain models in the SCOP++ environment. In: *Proceedings of OEEPE Workshop on Airborne Laserscanning and Interferometric SAR for Detailed Digital Terrain Models, Stockholm, Sweden*.

- Riegl, 2009a. [www.riegl.com](http://www.riegl.com). Homepage of the company RIEGL Laser Measurement Systems GmbH, accessed: October 2009.
- Riegl, 2009b. [www.riegl.com](http://www.riegl.com). Datasheet of the commercial full-waveform analyzing software RiAnalyze by RIEGL GmbH, accessed: November 2009.
- Roncat, A., Wagner, W., Melzer, T. and Ullrich, A., 2008. Echo detection and localization in full-waveform airborne laser scanner data using the averaged square difference function estimator. *The Photogrammetric Journal of Finland* 21(1), pp. 62–75.
- SCOP++, 2008. Institute of photogrammetry and remote sensing. [www.ipf.tuwien.ac.at/products/products.html](http://www.ipf.tuwien.ac.at/products/products.html).
- Tóvari, D. and Pfeifer, N., 2005. Segmentation based robust interpolation - a new approach to laser data filtering. In: *International Archives of Photogrammetry and Remote Sensing*, XXXVI, 3/W19, Enschede, The Netherlands, pp. 79–84.
- Vosselman, G., 2000. Slope based filtering of laser altimetry data. In: *International Archives of Photogrammetry and Remote Sensing*, XXXIII, B3, Amsterdam, Netherlands, pp. 935–942.
- Wagner, W., Hollaus, M., Briese, C. and Ducic, V., 2008. 3d vegetation mapping using small-footprint full-waveform airborne laser scanners. *International Journal of Remote Sensing* Vol. 29, No. 5, pp. 1433–1452.
- Wagner, W., Ullrich, A., Ducic, V., Melzer, T. and Studnicka, N., 2006. Gaussian decomposition and calibration of a novel small-footprint full-waveform digitising airborne laser scanner. *ISPRS Journal of Photogrammetry and Remote Sensing* 60(2), pp. 100–112.
- Wagner, W., Ullrich, A., Melzer, T., Briese, C. and Kraus, K., 2004. From single-pulse to full-waveform airborne laser scanners: potential and practical challenges. In: *International Archives of Photogrammetry and Remote Sensing*, XXXV, Istanbul, Turkey.